HHS Public Access

Author manuscript

FEBS J. Author manuscript; available in PMC 2022 June 01.

Published in final edited form as:

FEBS J. 2021 June ; 288(11): 3585–3601. doi:10.1111/febs.15683.

Phagocytic activity of splenic macrophages is enhanced and accompanied by cytosolic alkalinization in TRPM7 kinase-dead mice

Pavani Beesetty[1,*], **Jananie Rockwood**[1,*], **Taku Kaitsuka**[2], **Tetyana Zhelay**[1], **Siham Hourani**[1], **Masayuki Matsushita**[3], **J. Ashot Kozak**[1,#]

[1]Department of Neuroscience, Cell Biology and Physiology, Boonshoft School of Medicine and College of Science and Mathematics, Wright State University, Dayton, OH 45435, USA

[2]Department of Molecular Physiology, Faculty of Life Sciences, Kumamoto University, Kumamoto, Japan

[3]Department of Molecular and Cellular Physiology, Graduate School of Medicine, University of the Ryukyus, Okinawa 903-0215, Japan.

Abstract

Transient receptor potential melastatin 7 (TRPM7) is a unique protein functioning as a cation channel as well as a serine/threonine kinase and is highly expressed in immune cells such as lymphocytes and macrophages. TRPM7 kinase-dead (KD) mouse model has been used to investigate the role of this protein in immune cells; these animals display moderate splenomegaly and ectopic hemopoiesis. The basal TRPM7 current magnitudes in peritoneal macrophages isolated from KD mice were higher, however the maximum currents, achieved after cytoplasmic Mg^{2+} washout were not different. In the present study, we investigated the consequences of TRPM7 kinase inactivation in splenic and peritoneal macrophages. We measured the basal phagocytic activity of splenic macrophages using fluorescent latex beads, pHrodo zymosan bioparticles and opsonized red blood cells. KD macrophages phagocytized more efficiently and had slightly higher baseline calcium levels compared to WT cells. We found no obvious differences in store-operated Ca^{2+} entry between WT and KD macrophages. By contrast, the resting cytosolic pH in KD macrophages was significantly more alkaline than in WT. Pharmacological blockade of sodium-hydrogen exchanger 1 (NHE1) reversed the cytosolic alkalinization and reduced phagocytosis in KD macrophages. Basal TRPM7 channel activity in KD macrophages was also reduced after NHE1 blockade. Cytosolic Mg^{2+} sensitivity of TRPM7 channels measured in peritoneal macrophages was similar in WT and KD mice. The higher basal TRPM7 channel activity in KD macrophages is likely due to alkalinization. Our results identify a novel role for TRPM7 kinase as a suppressor of basal phagocytosis and a regulator of cellular pH.

[#]corresponding author Biological Sciences Building II, Rm. 251, Wright State University, 3640 Colonel Glenn Hwy, Dayton, OH 45435, USA, juliusz.kozak@wright.edu.

[*]equal contributors

Author contributions

JAK designed the study. PB, JR, TK, TZ, SH, JAK performed experiments. MM provided transgenic mice. PB, JR, TK, TZ, SH, JAK analyzed data. PB, JR and JAK wrote manuscript.

Conflict of Interest

The authors declare no conflict of interest.

Keywords

ion channel; erythrophagocytosis; spleen; alkalinization; SLC9A1

Introduction

Macrophages play an essential role in innate and adaptive immune responses [1–4]. Resident macrophages, found in the lungs, adipose tissue, spleen, bone marrow, brain, peritoneal cavity and other parts of the body, play multiple roles, which include clearance of pathogens and senescent cells and antigen presentation [5, 6].

The spleen is involved in blood homeostasis, and is home to a heterogeneous population of macrophages localized to red pulp, marginal zone and white pulp (tingible body) [7]. Red pulp macrophages phagocytize aged erythrocytes [6] and produce proinflammatory cytokines such as tumor necrosis factor alpha (TNF-α) and type 1 interferons (IFN) [8]. The marginal zone macrophages, including the metallophilic, play a crucial role in immune surveillance and priming the adaptive immune responses to bacterial and viral pathogens. Tingible body macrophages are responsible for the clearance of dead lymphocytes [6].

The ion channels of transient receptor potential (TRP) family play diverse roles in immune cell development and function [9, 10]. TRP channels expressed in macrophages and monocytes respond to exogenous stimuli from the environment such as heat, acidity and chemicals and also to signals produced endogenously due to trauma or tissue damage [9].

The channel-enzyme transient receptor potential melastatin-subfamily 7 (TRPM7) is highly expressed in immune cells, including T-cells, mast cells and macrophages (e.g. [11–15]). The channel portion of this protein is permeable to divalent metal cations such as Ca^{2+}, Mg^{2+} and Zn^{2+} [16, 17] and, at the same time, is inhibited by these cations from inside [18–20]. TRPM7 channels are also inhibited by polyamines and protons [14, 19]. This voltage-independent inhibition by cytosolic cations takes place through electrostatic screening and sequestration of phosphoinositides [19, 21]. TRPM7 channel biophysical characteristics are modified by extracellular calcium and magnesium: in their absence the current-voltage (I-V) relationship is semi-linear, whereas in their presence it is steeply outwardly rectifying [15, 22]. The cytoplasmic C-terminal portion contains an atypical serine/threonine kinase [23, 24], which phosphorylates TRPM7 itself and exogenous substrates phospholipase Cγ (PLCγ), annexin A1, myosin IIA-C and eukaryotic elongation factor-2 kinase (eEF-2k) [24–28]. Mice heterozygous for kinase domain deletion exhibited hypomagnesemia and a defect in intestinal Mg^{2+} absorption, suggesting a role for TRPM7 in magnesium homeostasis, whereas homozygous kinase deletion resulted in embryonic lethality [29, 30]. The importance of TRPM7 in magnesium homeostasis has been questioned, however (see [31]). TRPM7 kinase inactivation alone did not alter serum total Mg^{2+} and Ca^{2+} levels [12].

The global TRPM7 kinase-dead (KD) mouse model was generated by introducing a lysine to arginine substitution (K1646R) in the Mg-ATP binding pocket and abolishing kinase activity [12]. Previous work from our group established that TRPM7 protein is upregulated during T-cell activation, and kinase activity is important for store-operated calcium entry (SOCE),

blastogenesis, and T-cell proliferation [11] (but see [32]). KD mice exhibit moderate splenomegaly and ectopic hemopoiesis [11]. Interestingly, in KD mouse peritoneal macrophages, basal TRPM7 channel activity was higher than in WT cells even though the protein expression levels were similar in both [12]. The mechanism underlying this higher basal channel activity remains unexplored.

The main focus of the present study are the consequences of TRPM7 kinase inactivation in splenic and peritoneal macrophages. WT and KD macrophages were identified as $F4/80^{+}CD11b^{+}CD68^{+}MOMA\text{-}2^{+}CD209b^{+}CD80^{+}CD14^{low}CD169^{\mathbf{high}}CD86^{\mathbf{low}}$ and $F4/80^{+}CD11b^{+}CD68^{+}MOMA\text{-}2^{+}CD209b^{+}CD80^{+}CD14^{low}CD169^{\mathbf{low}}CD86^{\mathbf{low}}$, respectively. Therefore, a large subset are classified as red pulp and marginal zone macrophages. Phagocytosis was used to examine the biological function of splenic macrophages *in vitro*: TRPM7 KD macrophages phagocytized latex beads, pHrodo zymosan particles and opsonized sheep red blood cells more efficiently compared to WT. The results presented here reveal a previously unknown TRPM7 kinase function as a suppressor of phagocytosis. The ubiquitous second messenger calcium regulates various immune cell functions including phagocytosis (reviewed in [2]). Although, KD macrophages had somewhat elevated basal cytosolic calcium levels, removal of extracellular calcium did not abrogate phagocytic activity and SOCE in murine macrophages was generally smaller compared to lymphocytes from the same mouse model [11]. No significant differences in TRPM7 channel Mg^{2+} sensitivity was detected in WT and KD peritoneal macrophages. In KD macrophages, cytosolic pH was significantly more alkaline than in WT. Pharmacologic blockade of sodium-hydrogen exchanger 1 (NHE1), the main NHE isoform expressed in macrophages, reversed the alkalinization and decreased basal channel activity and phagocytosis, suggesting that higher pH in KD cells stimulates TRPM7 channels. Importantly, NHE1 blockade also abolished the difference between WT and KD macrophage phagocytic activities. In conclusion, macrophages isolated from spleens of TRPM7 KD mice phagocytize more efficiently compared to WT through a mechanism that likely involves cytosolic alkalinization but is largely independent of Ca^{2+}.

Results

Macrophages isolated from TRPM7 kinase-dead mouse spleens express high levels of F4/80, CD11b and CD209b

Global TRPM7 kinase inactivation resulted in mice with enlarged spleens and their T cells showed reduced blastogenesis and proliferation [11]. In addition to lymphocytes, several resident macrophage populations are found in the spleen. Red pulp macrophages are involved in erythrocyte clearance and iron metabolism [6]. These cells are classically classified as $F4/80^{+}$, $CD209^{+}$, Dectin-2^{+} and Spi-C^{+} [6, 33]. Outer marginal zone macrophages are involved in immune surveillance and are $CD68^{+}$, $CD209b^{+}$, MARCO+, Dectin-2^{+} and $Tim4^{+}$. Inner marginal zone metallophilic macrophages are $CD68^{+}$ and $CD169^{+}$ and are also involved in immune surveillance. Germinal center macrophages, also known as white pulp macrophages, are involved in the clearance of apoptotic cells formed during the germinal center reaction and are classified as $CD68^{+}$ [6, 33].

For isolation of macrophages, cells from mechanically disrupted spleens were cultured for 6 days in RPMI-1640 as described in Materials and Methods and analyzed by flow cytometry to characterize their phenotype (Fig. 1). Both WT and KD cells expressed high levels of the glycoprotein F4/80, the macrophage lysosomal marker CD68, co-stimulatory molecule CD80 and intracellular macrophage and monocyte marker MOMA-2 [34], suggesting that our procedure yielded a relatively pure macrophage preparation. The lipopolysaccharide (LPS) binding protein CD14 and the surface marker CD86 were expressed at low levels in both WT and KD macrophages [34, 35]. F4/80 and the intracellular marker CD169 (also known as Siglec-1) were expressed at higher levels in WT compared to KD macrophages [34]. The surface marker CD11b and C-type lectin receptor CD209b (also known as DC-SIGN) [34] were expressed at higher levels in KD compared to WT macrophages. The expression levels of these markers indicated that our culturing technique is effective in isolating macrophages that are primarily from the red pulp and marginal zone regions. Since these macrophage populations are involved in immune surveillance and erythrocyte clearance, we next examined their phagocytic activity [36].

Splenic macrophages from TRPM7 KD mice phagocytize more efficiently than those from WT littermates

Phagocytic activity was assessed using latex beads, zymosan (pHrodo) bioparticles and opsonized red blood cells (RBCs) (Fig. 2). Macrophages were incubated with latex particles for 1–2 hours. KD mouse macrophages had a higher number of associated latex particles compared to WT. After 1 hour, KD macrophages phagocytized 2 latex beads more efficiently compared to WT ($p<0.1$). After 2 hours, there was a significant difference in phagocytosis of 1 latex bead between KD macrophages and WT ($p<0.05$). It was not determined, however, if in this assay the latex beads were internalized or simply attached to the cell surface [37].

To distinguish particles that have been phagocytized from those residing on the cell surface, we used pHrodo-conjugated zymosan bioparticles (Fig. 2). Acidic pH of the phagosome causes the phagocytized particles to fluoresce [38], allowing a more accurate quantification of bona fide phagocytized particles (Fig. 2D, E). Again, we observed higher phagocytosis by KD macrophages compared to WT.

RBCs were used to examine phagocytosis of a biologically relevant substrate. Splenic macrophages were incubated with opsonized sheep RBCs at various ratios, for 1 hour and phagocytosis was quantified using a plate reader assay. KD splenic macrophages phagocytized most efficiently at RBC to macrophage ratios of 50:1, 40:1 and 30:1 (Fig. 2F). Overall, KD splenic macrophages were more efficient than WT in all three phagocytosis assays which could be reflective of a mechanism that is no longer suppressed by TRPM7 kinase-mediated phosphorylation.

Magnesium and calcium ions in phagocytosis of zymosan bioparticles

The role of Ca^{2+} in phagocytosis has been addressed in many studies (reviewed in [2, 10]). For instance, the removal of cytosolic Ca^{2+} in murine macrophages reduced phagocytosis of serum-opsonized erythrocytes, IgG-opsonized and unopsonized latex beads [39–42].

However, other studies reported that low cytosolic Ca^{2+} levels did not impair phagocytosis of erythrocytes [43–45].

In order to compare the cytosolic Ca^{2+} levels in splenic macrophages from TRPM7 KD and WT mice, we used the ratiometric calcium indicator Fura-2 (Fig. 3). Live-cell fluorescence imaging in 4 mM external [Ca^{2+}], revealed that KD splenic macrophages have somewhat higher basal levels of Ca^{2+} compared to WT cells (Fig. 3A, B). In 2 mM [Ca^{2+}], this was not observed, however (Fig. 3C). We also measured SOCE by Ca^{2+} reintroducing following ER store depletion [46]. We did not find major differences in SOCE between WT and KD macrophages (Fig. 3A–C). The slight increase of SOCE in KD cells seen in Fig. 3A is likely due to the higher resting Ca^{2+} levels. Previous work done using the same TRPM7 KD mice showed that activated, but not resting splenocytes had lower basal Ca^{2+} compared to WT [11].

In order to examine if SOCE influenced phagocytosis, ER Ca^{2+} stores were depleted with CPA in RPMI medium to activate SOCE: this resulted in reduced zymosan particle phagocytosis in both WT and KD splenic macrophages (Fig. 3D). We then incubated the cells in presence of BTP2, an inhibitor of Orai channels [47]. Unexpectedly, BTP2 reduced phagocytosis further, preferentially in WT cells. BTP2 effect persisted in the absence of Ca^{2+} and Mg^{2+}, suggesting that it was independent of SOCE, and involved other cellular targets (Fig. 3D).

TRPM7 conducts Ca^{2+} and Mg^{2+} and the increased phagocytic efficiency observed in KD macrophages might indicate differences in the cellular response to Ca^{2+} or Mg^{2+} influx. We investigated the dependence of phagocytosis on external Ca^{2+} and Mg^{2+} individually, by incubating the cells in Ca^{2+} or Mg^{2+}-free Chelex-RPMI (Fig. 4). Phagocytosis was measured over 3 hours in the presence of 0.4 mM [Ca^{2+}] or [Mg^{2+}], close to concentrations of these ions in normal RPMI. The difference in phagocytic activity between WT and KD was reduced in the absence of Mg^{2+} but persisted in its presence (Fig. 4A–C and Fig. 3D). The difference between WT and KD was most pronounced in the presence of both Ca^{2+} and Mg^{2+} (Fig. 4). The observed difference in phagocytosis between WT and KD macrophages may depend more on Mg^{2+} than Ca^{2+} (Fig. 4A–C). The contribution of Ca^{2+} and Mg^{2+} entry to the KD phenotype will require further investigation. It should also be remembered that phagocytosis was measured in RPMI containing 0.42 Ca^{2+} and/or 0.4 Mg^{2+} (Fig. 4), whereas cytosolic Ca^{2+} levels were measured in 2 or 4 mM extracellular Ca^{2+} (Fig. 3).

TRPM7 protein levels, kinase activity and channel activity in splenic macrophages

An immunoblot (Fig. 5A) and a kinase assay (Fig. 5B) were performed to determine TRPM7 protein levels and kinase activity in WT and KD mouse splenic macrophages. As previously observed in peritoneal macrophages and splenic T cells [11, 12], moderate levels of TRPM7 protein were detected in splenic macrophages with TRPM7-specific antibody (Fig. 5A). TRPM7 kinase in WT macrophages was able to phosphorylate itself and the exogenous substrate myelin basic protein (MBP), by contrast no phosphorylation of TRPM7 or MBP was detected in KD macrophages (Fig. 5B).

Similar to peritoneal, WT and KD splenic macrophages expressed large TRPM7 currents (Fig. 5C). They also expressed substantial inwardly rectifying K^+ currents, considered a hallmark of macrophages originating in various tissues (e.g. [48–50]) (Fig. 5C). This potassium current is likely the main contributor to setting the resting membrane potential in these cells.

Detailed examination of Mg^{2+} sensitivity of kinase-inactivated TRPM7 channels.—In KD mouse peritoneal macrophages basal TRPM7 current magnitudes are increased, whereas maximum currents achieved after cytosolic Mg^{2+} washout are not different from WT [12]. The maximum current magnitude is a measure of the total number of functional channels and the basal (preactivated) current reflects the fraction of open channels in the intact cell [20]. One possible mechanism for the higher basal channel activity would be a lower Mg^{2+} sensitivity of the TRPM7 KD channels and reduced inhibition by Mg^{2+} present in an intact cell. We, therefore, characterized the channel Mg^{2+} sensitivity in detail in WT and KD peritoneal macrophages by whole cell patch-clamp, as described previously for Jurkat T cells [14]. Free internal Mg^{2+} concentrations of 0.399 – 303 μM were used for measuring TRPM7 current amplitudes (Fig. 5D) and the mean current densities (current normalized to cell capacitance) measured at 125th voltage ramp (~5 min) after the onset of recording were plotted. 5 minutes of recording is usually sufficient for the current to reach maximum magnitude (see Fig. 4 and [12]). TRPM7 current densities at 0.399, 7.3, 28.1, 145.2 and 303 μM [Mg^{2+}] were not significantly different between WT and KD macrophages. At 64.9 μM, KD TRPM7 channels displayed a significantly ($p<0.05$) stronger Mg^{2+} inhibition compared to WT. These data are in agreement with our previous finding that TRPM7 kinase activity does not play an important role in the sensitivity of TRPM7 channels to intracellular Mg^{2+} [12, 24], but differ from two studies that reported reduced Mg^{2+} sensitivity in murine embryonic fibroblasts (MEF) and peritoneal mast cells of KD mice [29, 32]. Based on our results, we conclude that the larger basal currents in KD macrophages cannot be explained by reduced inhibition of TRPM7 channels by cytosolic Mg^{2+}.

TRPM7 KD macrophage cytosolic pH is alkalinized: effects of NHE1 blockade on pH_i, basal channel activity and phagocytosis.—An alternative explanation for increased basal channel activity in KD macrophages would be a more alkaline cytosolic pH_i which is sufficient to activate TRPM7 currents even without Mg^{2+} depletion [14, 19]. Using the fluorescent pH indicator BCECF, cytosolic pH measurements in splenic macrophages revealed that resting KD macrophages were alkalinized (mean pH=7.85 ± 0.02) compared to WT (mean pH=7.58 ± 0.02) cells (Fig. 6A). Sodium-hydrogen exchangers are important players in setting the resting pH of macrophages and other phagocytes and their inhibition would be expected to prevent cytosolic alkalinization [51–54]. Pharmacological blockade of sodium-hydrogen exchanger 1 (NHE1) by cariporide (HOE 642) made the cytosolic pH of KD macrophages more acidic (pH=7.32 ± 0.02) ($p<0.0001$) (Fig. 6B). Cariporide effect on pH appeared more pronounced in KD splenic macrophages than in WT cells (Fig. 6C).

Expression of NHE1 (SLC9A1) but not NHE2, 3 (SLC9A2, A3) was detected by RT-PCR, performed on RNA isolated from WT and KD peritoneal macrophages (Fig. 6D). NHE1

transcript expression was similar in WT and KD macrophages. We then assessed the consequences of acidification on TRPM7 current magnitudes and the frequency of channel preactivation in KD peritoneal macrophages. Cytosolic acidification resulting from NHE inhibition by EIPA reduced basal TRPM7 currents and the frequency of current preactivation (Fig. 6E, F). Therefore, NHE blockade inhibits TRPM7 channel function in KD peritoneal macrophages, most likely by counteracting the alkalinization of the cytosol.

In order to test if the increased phagocytic activity of KD splenic macrophages was also a downstream consequence of alkalinization, pHrodo zymosan particle phagocytosis was measured in the presence and absence of 5 μM cariporide, to completely inhibit NHE1 transport [55]. At both 1 and 3 hours, cariporide abolished the difference between WT and KD macrophage phagocytic activity (Fig. 6G). In summary, these experiments demonstrate that cytosolic alkalization improves phagocytic capabilities, possibly by an indirect increase of TRPM7 channel activity (Fig. 6H). Furthermore, the inhibition of TRPM7 kinase also enhances phagocytosis, possibly through a mechanism that involves NHE1 (Fig. 2; Fig. 6G, H). Conversely, cytosolic acidification caused by NHE1 blockade results in decreased phagocytosis. Acidification also causes a decrease in TRPM7 current which could also contribute to reduced phagocytic ability of macrophages (Fig. 6H).

Discussion

The TRPM7 K1646R knock-in mouse model with inactivated kinase, has been instrumental in identifying the contribution of this domain to immune cell functions and development [11, 12]. In peritoneal macrophages from TRPM7 KD mice, the channel biophysical characteristics were unchanged, except for the basal activity, which was significantly higher than WT [12].

To our knowledge, the present study is the first that investigates the role of TRPM7 in splenic macrophages. Our experiments were performed on macrophages from the mouse spleen, cultured without adding growth factors such as macrophage colony-stimulating (M-CSF) [3, 5, 56]. By flow cytometry they were identified as F4/80^{+}CD11b^{+}CD68^{+}MOMA-2^{+}CD209b^{+}CD80^{+}CD14^{low}CD169^{low}CD86^{low} (Fig. 1). There were no statistically significant differences between WT and KD macrophages in regards to specific markers, and the majority are classified as red pulp and marginal zone macrophages based on their high F4/80, CD11b, CD209b expression [7]. The function of macrophages was assessed by performing *in vitro* phagocytosis assays. KD macrophages phagocytized latex beads, pHrodo zymosan bioparticles and opsonized sheep red blood cells more efficiently than those from WT mice (Fig. 2). Our results, therefore, reveal a novel function for TRPM7 kinase as a suppressor of basal phagocytosis.

Phagocytosis involves particle binding, actin assembly, membrane remodeling, pseudopod extension and phagosome closure [57]. All stages of phagocytosis from particle binding to clearance rely on ion fluxes, however, the specific ion channels involved are not fully characterized [10]. Several TRP channels have been linked to phagocytosis. Studies in TRPV1 knockout mice demonstrated that TRPV1 is required to protect against immune and inflammatory responses in the peritoneal cavity [58]. Knockout of TRPV1 was linked to

increased IL-1β, IL-6, IL-10 and TNF-α cytokine release, reduction in reactive oxygen species (ROS) and LPS-induced phagocytosis [58]. Genetic deletion or pharmacological blockade of TRPV2 caused defects in the early steps of phagocytosis, particle binding and internalization [59]. Phagocytosis of zymosan, IgG and complement-coated particle binding was impaired in macrophages from TRPV2 knockout mice. During phagocytosis, TRPV2 is recruited to the nascent phagosome and also depolarizes the plasma membrane [59]. In TRPM4 knockout mice, reduced mobilization of Ca^{2+} during septic peritonitis resulted in the inhibition of the Akt pathway, which subsequently reduced macrophage survival, bacterial phagocytosis and the release of proinflammatory cytokines IL-1β and TNF-α [60].

TRPM7 channels may play a role in polarization and proliferation of mouse bone marrow-derived macrophages (BMDM) [61]. Anti-inflammatory M2 macrophages had larger TRPM7 current densities compared to pro-inflammatory M1 macrophages. TRPM7 inhibitors, NS8593 and FTY20 (fingolimod) blocked proliferation of IL-4 and M-CSF induced macrophages [61]. Inhibition of TRPM7 by NS8593 and FTY20 prevented polarization of macrophages to M2 phenotype.

In the myeloid-specific deletion of TRPM7 (*LysM Cre*) mouse model it was found that TRPM7 channels are required for LPS-induced BMDM activation and increased intracellular Ca^{2+} [62]. These findings were further supported by experiments with FTY720: when TRPM7 channels were blocked, cytosolic Ca^{2+} elevations in response to LPS were diminished along with TLR4 endocytosis and downstream signaling. FTY720 phosphate, a FTY720 analog which does not block TRPM7 [63] or other known channel blockers were not tested in that study, however [62].

Here we demonstrate that in TRPM7 KD macrophages the cytosolic pH is significantly more alkaline, compared to wildtype cells (Fig. 6). Alkalinization results in increased basal channel activity, due to the pH dependence of TRPM7 [21]. Inhibition of NHE1, which extrudes protons in exchange for sodium ions, resulted in acidification and reduction in basal channel activity. Most strikingly, NHE1 inhibition also reduced phagocytosis (Fig. 6G). Thus, based on these results we conclude that increased phagocytic activity of KD mouse macrophages is caused by alkalinization and is reversed when pH_i is brought back to normal (Fig. 6H). In human peritoneal macrophages acidification impaired both TNF-α secretion and phagocytosis of zymosan [64] and in human neutrophils, *E. coli* phagocytosis in urine was suppressed by acidification [65]. In microglia it was demonstrated that activation by LPS or phorbol esters is accompanied by alkalinization and Ca^{2+} elevations and that NHE1 blockade abolished pH_i regulation [55]. NHE1 blockade also reduced microglial motility [66].

The increased phagocytic capability of TRPM7 KD macrophages is indicative of intracellular signaling events that require further exploration. In particular, TRPM7 kinase substrates and their role in phagocytosis need to be investigated. For example, phosphorylation by TRPM7 kinase of NHE1 or other transporters, which set the cytosolic pH in macrophages could be one mechanism of alkalinization [52]. It is important to mention, in this context, that NHE1 transcript expression levels did not depend on TRPM7 kinase (Fig. 6D). Annexin A1 and myosin II are two well-known substrates of TRPM7

kinase [4, 27, 67, 68]. Annexins are a group of actin-binding proteins that play a role in actin remodeling during phagocytosis [69]. Annexin A1 is found mostly in the cytosol, but also on the plasma membrane and in organelles such as phagosomes, endosomes and multivesicular bodies [69] [70]. Macrophages lacking the annexin A1 gene exhibit a defect in zymosan phagocytosis [70]. Annexin A1 is phosphorylated by TRPM7 kinase in a Ca^{2+}-dependent manner [26, 67]. In macrophages, annexin A1 binds to phagosomes containing latex beads in a Ca^{2+}- dependent manner [69]. In solutions where $CaCl_2$ was removed or maintained at 0.4 mM, we observed that TRPM7 KD macrophages consistently phagocytized pHrodo zymosan particles more efficiently than WT cells (Fig. 4). Our results suggest that the lack of TRPM7-dependent annexin A1 phosphorylation does not abolish its function in phagocytosis. Alternatively, phosphorylation of this protein can be rescued by other kinases such as protein kinase A, C and EGF kinase [71]. Therefore, the regulation of annexin A1 by TRPM7 kinase in the context of phagocytosis needs to be further explored. Myosin IIA, another TRPM7 kinase substrate, is mainly involved in ROS production and acidification of the phagosome [72]. RNAi knockdown of myosin IIA resulted in impaired phagosomal maturation but the uptake of latex beads and *E.coli* was not affected. The ability of RAW 264.7 cells to clear *E.coli* was reduced significantly in the absence of SHP-1, moesin or myosin IIA, which further supports a link between these proteins in phagosomal biogenesis [72]. It is unclear how the absence of TRPM7 kinase activity will contribute to the regulation of myosin IIA and if that will lead to increased phagocytosis.

The role of calcium during phagocytosis has been the subject of numerous studies (reviewed in [2] [10]). Several reports have found calcium to be required while others have discounted its role [4, 43, 44] [73]. Cytosolic calcium changes have been implicated in the development and function of macrophages [74]. TRPC1, Orai1, STIM1 complex was identified as a modulator of immune cell activation in response to ER stress. One mechanism of ER stress and unfolded protein response is suppression of SOCE. In the murine macrophage cell line RAW 264.7 and BMDMs, pharmacological inhibition of SOCE resulted in ER stress and increased inflammatory cytokine secretion and phagocytosis. Moreover, expression of TRPC1, Orai1 and STIM1 was downregulated under ER stress [74].

We measured basal Ca^{2+} and SOCE in splenic macrophages (Fig. 3). Calcium measurements in live cells showed that WT splenic macrophages had somewhat lower basal calcium levels than TRPM7 KD cells when measured in 4 mM but not in 2 mM Ca^{2+}. It remains unclear what the role of SOCE is in macrophage function (e.g. [75] [76]). In our hands, phagocytosis was somewhat reduced in cells incubated in CPA (Fig. 3D). SOCE blockade by BTP2 reduced phagocytosis, preferentially in WT cells (Fig. 3D). Since this effect persisted in the absence of external Ca^{2+}, it is likely not due to Orai channel blockade but an unrelated mechanism: one possibility would be the activation of TRPM4 [77], which is expressed in macrophages [60].

The consequences of altering calcium and magnesium homeostasis *in vitro* were investigated by Libako et al. (2016), using the murine macrophage cell line J774.E, finding that the concentration of extracellular magnesium did not affect endocytosis but low extracellular magnesium levels increased PMA-induced ROS production [78].

In macrophages, ion channels regulate cellular homeostasis and function. However, we have been unable to find in the literature specific mutations in ion channels other than TRPM7 that cause a gain-of-function phenotype as we describe here in TRPM7 KD splenic macrophages. Future studies will need to address the precise mechanism that is activated in the absence of TRPM7 kinase activity and improves phagocytic efficiency of macrophages and if this mechanism extends to other types of phagocytic cells. One interesting question that remains open is if increased basal TRPM7 channel activity is required for the increased phagocytosis (Fig. 6H). Another question is if splenomegaly observed in TRPM7 KD mice can be explained by increased volumes of macrophages caused by increased erythrophagocytosis. In summary, the presented findings support a unique role for TRPM7 kinase as a suppressor of basal phagocytosis, a regulator of cellular pH, and indirectly, of channel activity.

Materials and Methods

TRPM7 kinase-dead mice

TRPM7 kinase-dead mice were generated by a knock-in mutation K1646R [12]. Both WT and KD mice had a C57BL/6 background. Splenic macrophage experiments were performed on 2–6 months old male and female animals. All procedures involving animals were performed according to protocols approved by the Laboratory Animal Care and Use Committees of Wright State University, Kumamoto University and University of the Ryukyus conforming to the NIH guidelines.

Development of splenic macrophages

Mouse spleens were physically disrupted in 10 ml complete RPMI-1640 (Lonza, Walkersville, MD), supplemented with 2 mM L-glutamine, 10% fetal bovine serum (Thermo Fisher Scientific, Waltham, MA), 50 IU/ml penicillin and 50 μg/ml streptomycin (MP Biomedicals, Irvine, CA). The splenocyte suspension was passed through a 40 μm nylon cell strainer (Fisher Scientific, Fair Lawn, NJ) and cultured in a 100 × 15 mm petri dish (Fisher) in a 5% CO_2, 37ºC humidified incubator (Forma Scientific, Marietta, OH). After 3 days, the non-adherent cells were removed. On day 6, the culture supernatant was discarded and the adherent cells (largely splenic macrophages) were washed three times with Dulbecco's Ca^{2+}/Mg^{2+}-free phosphate-buffered saline (DPBS; HyClone, Logan, UT). After the last wash, 3 ml of Cellstripper non-enzymatic cell dissociation solution (Mediatech, Manassas, VA) was added and cells were incubated at 5% CO_2, 37ºC for 10 min on an orbital shaker. Macrophages were lifted by gentle pipetting and added to 10 ml ice-cold complete RPMI-1640. Cells were centrifuged at 350 g for 10 min and resuspended in media at the desired density. All the described experiments were performed using splenic macrophages differentiated for 6 days except for patch clamp experiments (see below).

Peritoneal macrophages were isolated as previously described in detail [12].

Flow cytometry analysis

Splenic macrophages were stained with fluorochrome-tagged antibodies against surface and internal markersF4/80, MOMA-2, CD68, CD11b, CD14, 209b, CD169, CD80 and CD-86 (Thermo Fisher Scientific).

Cells were incubated with FACS buffer containing Fc block (Mouse BD Fc Block; BD Pharmingen, San Diego, CA) for 5 min at 4°C. Fluorochrome-conjugated antibodies against surface markers were added to the samples and incubated for 30 min at 4°C in the dark. For staining intracellular markers, the cells were fixed, treated with Permeabilization Buffer (BD Pharmingen), incubated in mouse BD Fc block for 5 min and then stained with anti-MOMA-2 and anti-CD169 antibodies for 1 hour at room temperature. The cells were washed and analyzed on Accuri C6 Flow Cytometer (BD Accuri Cytometers, Ann Arbor, MI). Cell populations were analyzed using FlowJo software (Treestar Software, San Carlos, CA).

Phagocytosis assays

Phagocytosis assays were performed utilizing a) fluorescent latex beads, b) zymosan particles, and 3) opsonized sheep erythrocytes. Splenic macrophages were plated at a density of 1×10^5 cells per well in 96-well plates.

For latex bead phagocytosis assay, Fluoresbrite red 1 μm diameter microspheres (Polysciences, Warrington, PA) were added to splenic macrophages at 1:25 cell to bead ratio. Macrophages were incubated with latex beads in Live Cell Imaging Solution (Molecular Probes, Eugene, OR) for 1 or 2 hours at 37 °C. The cells were washed 3 times, fixed in 2% paraformaldehyde and images were taken using the EVOS cell imaging system (Life technologies, Grand Island, New York). The number of latex beads per cell were counted manually by two independent observers and results were plotted as histograms.

For phagocytosis assay with zymosan particles, 20 μl of reconstituted pHrodo red zymosan A Bioparticles (Molecular Probes) were added to the macrophages in live cell imaging solution at 37°C. Fluorescence measurements (Ex: 560 nm, Em: 590 nm) were taken using Synergy H1 hybrid plate reader (Biotek, Winooski, VT) every 30 min or 1 hour for 3 hours after the addition of particles to the cells. Only the internalized pHrodo red zymosan particles are expected to fluoresce due to the acidic pH of phagosomes [36].

Negative control wells were pre-incubated with 10 or 15 μM cytochalasin D (CytD) (Sigma-Aldrich, St. Louis, MO) for 30 min prior to the addition of pHrodo zymosan particles or latex beads, and the drug was present throughout the period of phagocytosis. For testing pharmacological blockers of SERCA, Orai channels and NHE1, the macrophages were pre-incubated in the presence of blockers for 30 minutes before adding pHrodo zymosan particles. Cariporide (HOE-642) (4-isopropyl-3-methylsulfonyl-benzoyl-guanidine-methanesulfonate) was from Santa Cruz Biotechnology (Dallas, TX), CPA (cyclopiazonic acid) was from EMD Millipore Corp (Burlington, MA), EIPA (5-N-ethyl-N-isopropyl amiloride) and BTP2 (YM-58483) were from Sigma-Aldrich. The drugs were present throughout the phagocytosis assay.

To characterize erythrophagocyosis, opsonized erythrocytes were used with CytoSelect 96-well phagocytosis assay kit (Cell Biolabs Inc, San Diego, CA) according to the manufacturer's instructions. Briefly, after plating splenic macrophages at 1×10^5 cells per well in 100 μl RPMI-1640 complete media in a 96-well plate, 1–3 months old sheep erythrocytes (Lampire Biological Laboratories, Pipersville, PA) were IgG opsonized on the day of experiment, and added at several macrophage to erythrocyte ratios (1:20, 1:30, 1:40 and 1:50). 5 μM CytD was added to negative control wells 1 hour before the addition of opsonized red blood cells at 1:50 ratio. After 1 hour of phagocytosis at 37ºC and 5% CO_2, non-phagocytized erythrocytes were aspirated, macrophages were lysed and red blood cells were quantitated using proprietary erythrocyte substrate by measuring absorbance at 630 nm after 15 min of substrate development using microtiter plate reader (Biotek).

In experiments where external divalent cations were removed (e.g. Fig. 3), RPMI-1640 medium was treated with Chelex-100 resin, as previously described [11, 20].

Patch-clamp electrophysiology

Murine peritoneal macrophages were isolated from WT and TRPM7 KD mice of all ages and used for whole-cell patch clamp electrophysiology as previously described [12]. The standard external (bathing) solution contained 2 mM $CaCl_2$, 140 mM Na Aspartate, 4.5 mM KCl, 3 mM CsCl, 10 mM HEPES.Na^+, 0.5 mM glucose, pH 7.3. The basic internal (pipette) solution contained 10 mM HEDTA, 106 mM glutamic acid, 5 mM CsF, 8 mM NaCl, 10 mM HEPES with pH adjusted to 7.3 with CsOH. This solution was supplemented with 0.06 – 7.74 mM $MgCl_2$ to yield calculated free [Mg^{2+}] of 0.399 – 303 μM [14]. For 303 μM free [Mg^{2+}], 7.74 mM $MgCl_2$ was added and the concentration of HEDTA and glutamic acid were reduced to 9 mM and 101 mM, respectively. For experiments involving NHE blockade, day 12–14 TRPM7 KD peritoneal macrophages were incubated with 20 μM EIPA for 24–48 hours (see Fig. 6).

TRPM7 currents in splenic macrophages were recorded as described above using cells that were grown on glass coverslips for up to 3 weeks. The extracellular solution contained 2 mM $CaCl_2$, 140 mM Na aspartate, 4.5 mM KCl, 3 mM CsCl, 10 mM HEPES, pH 7.3. Internal (pipette) Mg^{2+}-free solution contained 112 mM Cs glutamate, 10 mM HEDTA, 5 mM CsF, 10 mM HEPES, pH 7.3 with CsOH. 211 ms duration command voltage ramps from −100 to +85 mV were applied every 2 seconds and currents recorded and stored.

For recording the inwardly rectifying K^+ currents, KCl concentration in the external solution was increased to 30 mM by equimolar substitution of sodium aspartate and CsCl omitted. In the internal solution Cs glutamate was substituted with K glutamate. The internal solution contained 12 mM EGTA instead of HEDTA and 5 mM $MgCl_2$ to inhibit TRPM7 currents.

Instantaneous current-voltage relations and time courses of current development were plotted using Origin software (Origin Lab, Northampton, MA).

All electrophysiological measurements were performed at room temperature (24–25 ºC). Osmolalities of all recording solutions were measured using a freezing point osmometer and

adjusted with D-mannitol. All salts were purchased from Sigma-Aldrich, except HEPES-Na $^{+}$ and HEDTA which were from Acros Organics (Fairlawn, NJ).

Ratiometric Ca^{2+} measurement

Splenic macrophages used for calcium measurements were grown on 12 mm acid-washed coverslips in complete RPMI-1640. Ratiometric Ca^{2+} measurements were performed as previously described for T cells isolated from TRPM7 WT and KD mouse spleens [11]. The dye loading solution contained either 2 mM or 4 mM Ca^{2+} and Fura-2AM (Thermo Fisher Scientific), and cells were incubated in the presence of the dye at room temperature for 45 min followed by de-esterification for 15 min. The calcium-containing solution consisted of 2 mM or 4 mM $CaCl_2$, 140 mM NaCl, 4 mM KCl, 10 mM HEPES-Na^+, 10 mM glucose, pH 7.3, ~300 mOsm. The calcium-free solution contained 2 mM EGTA. CPA was used at 20 μM to deplete intracellular calcium stores. Ionomycin (EMD Millipore) was used as a dye loading control and added to the recording solutions at a concentration of 10 μM at the end of the experiment. Fura-2 fluorescence properties are not expected to be significantly affected by alkalinization in the range observed in KD macrophages (see Figure 6) [79]. A syringe-driven perfusion system was used to exchange the solutions in the glass-bottom imaging chamber placed on a mechanical stage of an inverted microscope (Olympus, Japan). Cells in the field of view were illuminated every 6 seconds at 340 nm and 380 nm wavelengths using a Lambda 10B shutter and filter wheel (Sutter Instrument, Novato, CA). The light source used was a 175 W Xenon lamp (Intracellular Imaging, Cincinnati, OH). Live-cell images were captured with a Pixelfly CCD camera (PCO Imaging, Kelheim, Germany) and InCyt Im 2 software (Intracellular Imaging). For individual cell Ca^{2+} measurements, 340 nm to 380 nm ratios were plotted using steady state levels achieved in each bathing solution.

Ratiometric pH measurement

Single-cell pH measurements were performed on splenic macrophages as previously described for Jurkat T cells [80]. Macrophages were grown on 12 mm acid-washed coverslips for 6 days in RPMI-1640 and the coverslips were transferred to a 35 mm glass-bottom imaging chamber with a solution volume of ~1 ml. Cells were loaded with 4 μM BCECF-AM ester (ThermoFisher) with 4 mM probenecid and 0.08% pluronic in the imaging solution for 45 minutes at 37°C followed by de-esterification for 15 minutes at room temperature. The standard imaging solution contained 2 mM $CaCl_2$, 140 mM NaCl, 4 mM KCl, 10 mM HEPES-Na^+, 10 mM glucose, pH 7.3. For measurements with NHE-1 inhibitors, macrophages were incubated for at least 4 hours in media containing 10 μM cariporde. Cariporide was also present during loading, de-esterification and imaging. For individual cell 3-point pH calibration, the cells were superfused with a high K^+ modified recording solution containing 1 mM $CaCl_2$, 20 mM NaCl, 130 mM KCl, 5 mM glucose, 0.5 mM $MgSO_4$, 1 mM NaH_2PO_4, 15 mM HEPES acid, 1 mM MES. Nigericin sodium salt (Sigma-Aldrich) was added to the high [K^+] solution at a final concentration of 10 μM and the pH adjusted to pH 6.5, 7.7 and 7.9, ~308 mOsm. Individual cells in the imaging field were illuminated every 6 seconds at 490 and 440 nm wavelengths using a Lambda 10B shutter and filter wheel (Sutter). Ratio measurements were calculated when the cell pH

reached steady state in a given solution. The emitted light intensities from individual cells were calculated and plotted using Origin software (v. 2018b).

Immunoblotting

Immunoblotting was performed as previously described for splenic T cells [11]. TRPM7 protein isolated from splenic macrophages was immunoprecipitated, and macrophage lysates were incubated with rabbit polyclonal anti-TRPM7 antibody (1:500) (AB15562; Millipore, Billerica, MA) overnight at 4°C, followed by incubation with protein A sepharose beads for 1 hour. The beads were then washed three times in lysis buffer. Protein bound to sepharose A beads was eluted using Laemmli sample buffer. SDS-PAGE analysis was performed on the eluted protein. PVDF membrane was used to transfer the protein from the SDS gel (Millipore) and blocked with Blocking One (Nacalai Tesque, Kyoto, Japan). The blocked membrane was probed with anti-TRPM7 antibody overnight at 4°C, washed, and incubated for 1 hour with the secondary HRP-conjugated anti-rabbit IgG (1:2000) antibody (Dako, Carpenteria, CA). The membrane was washed afterwards and incubated with Amersham ECL Prime (GE Healthcare, Piscataway, NJ). TRPM7 protein was visualized using ImageQuant400 (GE Healthcare).

Kinase Assay

Kinase assays on splenic macrophages were performed as previously described for T-cells and peritoneal macrophages [11, 12]. Splenic macrophages from WT and TRPM7 KD mice were lysed in lysis buffer (50 mM Tris-HCl, pH 7.5, 120 mM NaCl, 0.5 mM DTT, 1.5 mM $MgCl_2$, 0.2 mM EDTA, 1% Triton X-100 supplemented with protease inhibitors) on ice for 20 min. The cell lysates were centrifuged for 10 min at 20,000 g to remove insoluble material. Cell extracts were incubated overnight at 4°C with anti-TRPM7 antibody (1:500) (AB15562, Millipore), followed by incubation with protein A sepharose beads for 1 hour. The beads were then washed three times in lysis buffer, followed by one wash in the kinase buffer (50 mM HEPES, pH 7.0, 4 mM $MnCl_2$, 5 mM DTT), and resuspended in 50 μl kinase buffer. Myelin basic protein (MBP) substrate (50 μg/ml) was added to the immunoprecipitate. The phosphotransferase reaction was initiated with 0.1 mM ATP and 5 μCi [$\gamma-^{32}$P] ATP. After a 30 minutes reaction at 30°C, Laemmli sample buffer was used to elute the proteins bound to the beads. Proteins were separated using SDS-PAGE, and phosphate incorporation was evaluated by autoradiography.

RT-PCR

The peritoneal macrophages and kidney tissue were lysed and homogenized in TRIzol reagent (Ambion, Austin, TX) to isolate total RNA. RT-PCR was performed using Verso 1-step RT-PCR kit (Thermo Scientific) with specific sets of primers essentially as previously described [20]. The primer sets used were: GAPDH Fwd 5'-AGGCCGGTGCTGAGTATGTC-3'/ Rev 5'-TGCCTGCTTCACCACCTTCT-3', NHE1 Fwd 5'- CTGTGGTCATTATGGCC-3'/ Rev 5'- TGGGTTCATAGGCCAGT-3', NHE2 Fwd 5'- CAGCAAGCTGTCAGTGA-3'/ Rev 5'-TCGGGAGGTTGAAGTGG-3', NHE3 Fwd 5'-TGTATATCGAGCCATTGGTGT-3'/ Rev 5'- CTTCAAATTCAGCTCATGGAA-3'. For each reaction ~250 ng of total RNA was used and 35 PCR cycles were performed for

peritoneal macrophage RNA and 38 cycles for kidney RNA (Thermocycler 2720, Applied Biosystems (Foster City, CA).

Acknowledgements

We thank Emily Nolan and Rikki Chokshi for technical assistance, Dr. Lucy Wrenshall for the use of EVOS microscope and Biotek plate reader and Michael Bottomley, Statistical Consulting Center, Wright State University for help with statistical analysis. This work was supported by NIAID 1R01AI114804 (to JAK). SH was supported in part by NIH R25 GM086257 GRAD-PREP Biomedical Graduate Preparation Program.

Abbreviations

TRPM7	transient receptor potential melastatin 7
KD	kinase-dead
RBC	red blood cell
SOCE	store-operated calcium entry
NHE1–3	sodium-hydrogen exchanger 1–3
SERCA	sarco/endoplasmic reticulum calcium ATPase
CPA	cyclopiazonic acid

References

1. Fujiyama S, Nakahashi-Oda C, Abe F, Wang Y, Sato K & Shibuya A (2019) Identification and isolation of splenic tissue-resident macrophage sub-populations by flow cytometry, Int Immunol. 31, 51–56. [PubMed: 30256964]
2. Nunes-Hasler P, Kaba M & Demaurex N (2020) Molecular Mechanisms of Calcium Signaling During Phagocytosis, Advances in experimental medicine and biology. 1246, 103–128. [PubMed: 32399828]
3. Alatery A & Basta S (2008) An efficient culture method for generating large quantities of mature mouse splenic macrophages, J Immunol Methods. 338, 47–57. [PubMed: 18675819]
4. Nadolni W & Zierler S (2018) The Channel-Kinase TRPM7 as Novel Regulator of Immune System Homeostasis, Cells. 7.
5. Wang C, Yu X, Cao Q, Wang Y, Zheng G, Tan TK, Zhao H, Zhao Y, Wang Y & Harris D (2013) Characterization of murine macrophages from bone marrow, spleen and peritoneum, BMC Immunol. 14, 6. [PubMed: 23384230]
6. Davies LC, Jenkins SJ, Allen JE & Taylor PR (2013) Tissue-resident macrophages, Nature immunology. 14, 986–95. [PubMed: 24048120]
7. Borges da Silva H, Fonseca R, Pereira RM, Cassado Ados A, Alvarez JM & D'Imperio Lima MR (2015) Splenic Macrophage Subsets and Their Function during Blood-Borne Infections, Frontiers in immunology. 6, 480. [PubMed: 26441984]
8. Kim CC, Nelson CS, Wilson EB, Hou B, DeFranco AL & DeRisi JL (2012) Splenic red pulp macrophages produce type I interferons as early sentinels of malaria infection but are dispensable for control, PloS one. 7, e48126. [PubMed: 23144737]
9. Santoni G, Morelli MB, Amantini C, Santoni M, Nabissi M, Marinelli O & Santoni A (2018) "Immuno-Transient Receptor Potential Ion Channels": The Role in Monocyte- and Macrophage-Mediated Inflammatory Responses, Frontiers in immunology. 9, 1273. [PubMed: 29928281]
10. Feske S, Wulff H & Skolnik EY (2015) Ion channels in innate and adaptive immunity, Annual review of immunology. 33, 291–353.

11. Beesetty P, Wieczerzak KB, Gibson JN, Kaitsuka T, Luu CT, Matsushita M & Kozak JA (2018) Inactivation of TRPM7 kinase in mice results in enlarged spleens, reduced T-cell proliferation and diminished store-operated calcium entry, Scientific reports. 8, 3023. [PubMed: 29445164]
12. Kaitsuka T, Katagiri C, Beesetty P, Nakamura K, Hourani S, Tomizawa K, Kozak JA & Matsushita M (2014) Inactivation of TRPM7 kinase activity does not impair its channel function in mice, Scientific reports. 4, 5718. [PubMed: 25030553]
13. Huang L, Ng NM, Chen M, Lin X, Tang T, Cheng H, Yang C & Jiang S (2014) Inhibition of TRPM7 channels reduces degranulation and release of cytokines in rat bone marrow-derived mast cells, International journal of molecular sciences. 15, 11817–31. [PubMed: 24995695]
14. Chokshi R, Matsushita M & Kozak JA (2012) Detailed examination of Mg2+ and pH sensitivity of human TRPM7 channels, American journal of physiology Cell physiology. 302, C1004–11. [PubMed: 22301056]
15. Kozak JA, Kerschbaum HH & Cahalan MD (2002) Distinct properties of CRAC and MIC channels in RBL cells, The Journal of general physiology. 120, 221–35. [PubMed: 12149283]
16. Monteilh-Zoller MK, Hermosura MC, Nadler MJ, Scharenberg AM, Penner R & Fleig A (2003) TRPM7 provides an ion channel mechanism for cellular entry of trace metal ions, The Journal of general physiology. 121, 49–60. [PubMed: 12508053]
17. Chubanov V, Mittermeier L & Gudermann T (2018) Role of kinase-coupled TRP channels in mineral homeostasis, Pharmacology & therapeutics. 184, 159–176. [PubMed: 29129644]
18. Kozak JA & Cahalan MD (2003) MIC channels are inhibited by internal divalent cations but not ATP, Biophysical journal. 84, 922–7. [PubMed: 12547774]
19. Kozak JA, Matsushita M, Nairn AC & Cahalan MD (2005) Charge screening by internal pH and polyvalent cations as a mechanism for activation, inhibition, and rundown of TRPM7/MIC channels, The Journal of general physiology. 126, 499–514. [PubMed: 16260839]
20. Mellott A, Rockwood J, Zhelay T, Luu CT, Kaitsuka T & Kozak JA (2020) TRPM7 channel activity in Jurkat T lymphocytes during magnesium depletion and loading: implications for divalent metal entry and cytotoxicity, Pflugers Archiv : European journal of physiology. 472, 1589–1606. [PubMed: 32964285]
21. Zhelay T, Wieczerzak KB, Beesetty P, Alter GM, Matsushita M & Kozak JA (2018) Depletion of plasma membrane-associated phosphoinositides mimics inhibition of TRPM7 channels by cytosolic Mg(2+), spermine, and pH, The Journal of biological chemistry. 293, 18151–18167. [PubMed: 30305398]
22. Chokshi R, Matsushita M & Kozak JA (2012) Sensitivity of TRPM7 channels to Mg2+ characterized in cell-free patches of Jurkat T lymphocytes, American journal of physiology Cell physiology. 302, C1642–51. [PubMed: 22460708]
23. Yamaguchi H, Matsushita M, Nairn AC & Kuriyan J (2001) Crystal structure of the atypical protein kinase domain of a TRP channel with phosphotransferase activity, Molecular cell. 7, 1047–57. [PubMed: 11389851]
24. Matsushita M, Kozak JA, Shimizu Y, McLachlin DT, Yamaguchi H, Wei FY, Tomizawa K, Matsui H, Chait BT, Cahalan MD & Nairn AC (2005) Channel function is dissociated from the intrinsic kinase activity and autophosphorylation of TRPM7/ChaK1, The Journal of biological chemistry. 280, 20793–803. [PubMed: 15781465]
25. Deason-Towne F, Perraud AL & Schmitz C (2012) Identification of Ser/Thr phosphorylation sites in the C2-domain of phospholipase C gamma2 (PLCgamma2) using TRPM7-kinase, Cellular signalling. 24, 2070–5. [PubMed: 22759789]
26. Dorovkov MV, Kostyukova AS & Ryazanov AG (2011) Phosphorylation of annexin A1 by TRPM7 kinase: a switch regulating the induction of an alpha-helix, Biochemistry. 50, 2187–93. [PubMed: 21280599]
27. Clark K, Middelbeek J, Dorovkov MV, Figdor CG, Ryazanov AG, Lasonder E & van Leeuwen FN (2008) The alpha-kinases TRPM6 and TRPM7, but not eEF-2 kinase, phosphorylate the assembly domain of myosin IIA, IIB and IIC, FEBS letters. 582, 2993–7. [PubMed: 18675813]
28. Perraud AL, Zhao X, Ryazanov AG & Schmitz C (2011) The channel-kinase TRPM7 regulates phosphorylation of the translational factor eEF2 via eEF2-k, Cellular signalling. 23, 586–93. [PubMed: 21112387]

29. Ryazanova LV, Rondon LJ, Zierler S, Hu Z, Galli J, Yamaguchi TP, Mazur A, Fleig A & Ryazanov AG (2010) TRPM7 is essential for Mg(2+) homeostasis in mammals, Nature communications. 1, 109.
30. Rios FJ, Zou ZG, Harvey AP, Harvey KY, Nosalski R, Anyfanti P, Camargo LL, Lacchini S, Ryazanov AG, Ryazanova L, McGrath S, Guzik TJ, Goodyear CS, Montezano AC & Touyz RM (2020) Chanzyme TRPM7 protects against cardiovascular inflammation and fibrosis, Cardiovascular research. 116, 721–735. [PubMed: 31250885]
31. Jin J, Desai BN, Navarro B, Donovan A, Andrews NC & Clapham DE (2008) Deletion of Trpm7 disrupts embryonic development and thymopoiesis without altering Mg2+ homeostasis, Science. 322, 756–60. [PubMed: 18974357]
32. Romagnani A, Vettore V, Rezzonico-Jost T, Hampe S, Rottoli E, Nadolni W, Perotti M, Meier MA, Hermanns C, Geiger S, Wennemuth G, Recordati C, Matsushita M, Muehlich S, Proietti M, Chubanov V, Gudermann T, Grassi F & Zierler S (2017) TRPM7 kinase activity is essential for T cell colonization and alloreactivity in the gut, Nature communications. 8, 1917.
33. Kurotaki D, Uede T & Tamura T (2015) Functions and development of red pulp macrophages, Microbiol Immunol. 59, 55–62. [PubMed: 25611090]
34. Dos Anjos Cassado A (2017) F4/80 as a Major Macrophage Marker: The Case of the Peritoneum and Spleen, Results Probl Cell Differ. 62, 161–179. [PubMed: 28455709]
35. Orecchioni M, Ghosheh Y, Pramod AB & Ley K (2019) Macrophage Polarization: Different Gene Signatures in M1(LPS+) vs. Classically and M2(LPS−) vs. Alternatively Activated Macrophages, Frontiers in immunology. 10.
36. Bronte V & Pittet MJ (2013) The spleen in local and systemic regulation of immunity, Immunity. 39, 806–18. [PubMed: 24238338]
37. Sulahian TH, Imrich A, Deloid G, Winkler AR & Kobzik L (2008) Signaling pathways required for macrophage scavenger receptor-mediated phagocytosis: analysis by scanning cytometry, Respiratory research. 9, 59. [PubMed: 18687123]
38. Surewaard BGJ & Kubes P (2017) Measurement of bacterial capture and phagosome maturation of Kupffer cells by intravital microscopy, Methods. 128, 12–19. [PubMed: 28522327]
39. Young JD, Ko SS & Cohn ZA (1984) The increase in intracellular free calcium associated with IgG gamma 2b/gamma 1 Fc receptor-ligand interactions: role in phagocytosis, Proceedings of the National Academy of Sciences of the United States of America. 81, 5430–4. [PubMed: 6236462]
40. Hishikawa T, Cheung JY, Yelamarty RV & Knutson DW (1991) Calcium transients during Fc receptor-mediated and nonspecific phagocytosis by murine peritoneal macrophages, The Journal of cell biology. 115, 59–66. [PubMed: 1918139]
41. Ichinose M, Asai M & Sawada M (1995) beta-Endorphin enhances phagocytosis of latex particles in mouse peritoneal macrophages, Scand J Immunol. 42, 311–6. [PubMed: 7660064]
42. Ichinose M, Asai M, Imai K & Sawada M (1995) Enhancement of phagocytosis in mouse macrophages by pituitary adenylate cyclase activating polypeptide (PACAP) and related peptides, Immunopharmacology. 30, 217–24. [PubMed: 8557521]
43. McNeil PL, Swanson JA, Wright SD, Silverstein SC & Taylor DL (1986) Fc-receptor-mediated phagocytosis occurs in macrophages without an increase in average [Ca++]i, The Journal of cell biology. 102, 1586–92. [PubMed: 3700467]
44. Di Virgilio F, Meyer BC, Greenberg S & Silverstein SC (1988) Fc receptor-mediated phagocytosis occurs in macrophages at exceedingly low cytosolic Ca2+ levels, The Journal of cell biology. 106, 657–66. [PubMed: 3346321]
45. Greenberg S, el Khoury J, di Virgilio F, Kaplan EM & Silverstein SC (1991) Ca(2+)-independent F-actin assembly and disassembly during Fc receptor-mediated phagocytosis in mouse macrophages, The Journal of cell biology. 113, 757–67. [PubMed: 2026648]
46. Bird GS, DeHaven WI, Smyth JT & Putney JW Jr. (2008) Methods for studying store-operated calcium entry, Methods. 46, 204–12. [PubMed: 18929662]
47. Bogeski I, Al-Ansary D, Qu B, Niemeyer BA, Hoth M & Peinelt C (2010) Pharmacology of ORAI channels as a tool to understand their physiological functions, Expert review of clinical pharmacology. 3, 291–303. [PubMed: 22111611]

48. Randriamampita C & Trautmann A (1987) Ionic channels in murine macrophages, The Journal of cell biology. 105, 761–769. [PubMed: 2442173]
49. Kettenmann H, Hoppe D, Gottmann K, Banati R & Kreutzberg G (1990) Cultured microglial cells have a distinct pattern of membrane channels different from peritoneal macrophages, Journal of neuroscience research. 26, 278–87. [PubMed: 1697905]
50. Moreno C, Prieto P, Macias A, Pimentel-Santillana M, de la Cruz A, Traves PG, Bosca L & Valenzuela C (2013) Modulation of voltage-dependent and inward rectifier potassium channels by 15-epi-lipoxin-A4 in activated murine macrophages: implications in innate immunity, Journal of immunology. 191, 6136–46.
51. Grinstein S, Swallow CJ & Rotstein OD (1991) Regulation of cytoplasmic pH in phagocytic cell function and dysfunction, Clinical biochemistry. 24, 241–7. [PubMed: 1651820]
52. De Vito P (2006) The sodium/hydrogen exchanger: a possible mediator of immunity, Cellular immunology. 240, 69–85. [PubMed: 16930575]
53. Rotte A, Pasham V, Eichenmuller M, Mahmud H, Xuan NT, Shumilina E, Gotz F & Lang F (2010) Effect of bacterial lipopolysaccharide on Na(+)/H(+) exchanger activity in dendritic cells, Cellular physiology and biochemistry : international journal of experimental cellular physiology, biochemistry, and pharmacology. 26, 553–62.
54. Shi Y, Chanana V, Watters JJ, Ferrazzano P & Sun D (2011) Role of sodium/hydrogen exchanger isoform 1 in microglial activation and proinflammatory responses in ischemic brains, Journal of neurochemistry. 119, 124–35. [PubMed: 21797866]
55. Liu Y, Kintner DB, Chanana V, Algharabli J, Chen X, Gao Y, Chen J, Ferrazzano P, Olson JK & Sun D (2010) Activation of microglia depends on Na+/H+ exchange-mediated H+ homeostasis, The Journal of neuroscience : the official journal of the Society for Neuroscience. 30, 15210–20. [PubMed: 21068326]
56. Asakura E, Yamauchi T, Umemura A, Hanamura T & Tanabe T (1997) Intravenously administered macrophage colony-stimulating factor (M-CSF) specifically acts on the spleen, resulting in the increasing and activating spleen macrophages for cytokine production in mice, Immunopharmacology. 37, 7–14. [PubMed: 9285239]
57. Cox D & Greenberg S (2001) Phagocytic signaling strategies: Fc(gamma)receptor-mediated phagocytosis as a model system, Semin Immunol. 13, 339–45. [PubMed: 11708889]
58. Fernandes ES, Liang L, Smillie SJ, Kaiser F, Purcell R, Rivett DW, Alam S, Howat S, Collins H, Thompson SJ, Keeble JE, Riffo-Vasquez Y, Bruce KD & Brain SD (2012) TRPV1 deletion enhances local inflammation and accelerates the onset of systemic inflammatory response syndrome, Journal of immunology. 188, 5741–51.
59. Link TM, Park U, Vonakis BM, Raben DM, Soloski MJ & Caterina MJ (2010) TRPV2 has a pivotal role in macrophage particle binding and phagocytosis, Nature immunology. 11, 232–9. [PubMed: 20118928]
60. Serafini N, Dahdah A, Barbet G, Demion M, Attout T, Gautier G, Arcos-Fajardo M, Souchet H, Jouvin MH, Vrtovsnik F, Kinet JP, Benhamou M, Monteiro RC & Launay P (2012) The TRPM4 channel controls monocyte and macrophage, but not neutrophil, function for survival in sepsis, Journal of immunology. 189, 3689–99.
61. Schilling T, Miralles F & Eder C (2014) TRPM7 regulates proliferation and polarisation of macrophages, Journal of cell science. 127, 4561–6. [PubMed: 25205764]
62. Schappe MS, Szteyn K, Stremska ME, Mendu SK, Downs TK, Seegren PV, Mahoney MA, Dixit S, Krupa JK, Stipes EJ, Rogers JS, Adamson SE, Leitinger N & Desai BN (2018) Chanzyme TRPM7 Mediates the Ca(2+) Influx Essential for Lipopolysaccharide-Induced Toll-Like Receptor 4 Endocytosis and Macrophage Activation, Immunity. 48, 59–74.e5. [PubMed: 29343440]
63. Qin X, Yue Z, Sun B, Yang W, Xie J, Ni E, Feng Y, Mahmood R, Zhang Y & Yue L (2013) Sphingosine and FTY720 are potent inhibitors of the transient receptor potential melastatin 7 (TRPM7) channels, British journal of pharmacology. 168, 1294–312. [PubMed: 23145923]
64. Douvdevani A, Rapoport J, Konforty A, Yulzari R, Moran A & Chaimovitz C (1995) Intracellular acidification mediates the inhibitory effect of peritoneal dialysate on peritoneal macrophages, Journal of the American Society of Nephrology. 6, 207. [PubMed: 7579086]

65. Gargan RA, Hamilton-Miller JM & Brumfitt W (1993) Effect of pH and osmolality on in vitro phagocytosis and killing by neutrophils in urine, Infection and immunity. 61, 8–12. [PubMed: 8418067]
66. Shi Y, Yuan H, Kim D, Chanana V, Baba A, Matsuda T, Cengiz P, Ferrazzano P & Sun D (2013) Stimulation of Na(+)/H(+) exchanger isoform 1 promotes microglial migration, PloS one. 8, e74201. [PubMed: 23991215]
67. Dorovkov MV & Ryazanov AG (2004) Phosphorylation of annexin I by TRPM7 channel-kinase, The Journal of biological chemistry. 279, 50643–6. [PubMed: 15485879]
68. Clark K, Middelbeek J, Morrice NA, Figdor CG, Lasonder E & van Leeuwen FN (2008) Massive Autophosphorylation of the Ser/Thr-Rich Domain Controls Protein Kinase Activity of TRPM6 and TRPM7, PloS one. 3, e1876. [PubMed: 18365021]
69. Patel DM, Ahmad SF, Weiss DG, Gerke V & Kuznetsov SA (2011) Annexin A1 is a new functional linker between actin filaments and phagosomes during phagocytosis, Journal of cell science. 124, 578–88. [PubMed: 21245195]
70. D'Acquisto F, Perretti M & Flower RJ (2008) Annexin-A1: a pivotal regulator of the innate and adaptive immune systems, British journal of pharmacology. 155, 152–69. [PubMed: 18641677]
71. D'Acunto CW, Gbelcova H, Festa M & Ruml T (2014) The complex understanding of Annexin A1 phosphorylation, Cellular signalling. 26, 173–178. [PubMed: 24103589]
72. Gomez CP & Descoteaux A (2018) Moesin and myosin IIA modulate phagolysosomal biogenesis in macrophages, Biochemical and biophysical research communications. 495, 1964–1971. [PubMed: 29247647]
73. Demaurex N & Nunes P (2016) The role of STIM and ORAI proteins in phagocytic immune cells, American journal of physiology Cell physiology. 310, C496–508. [PubMed: 26764049]
74. Nascimento Da Conceicao V, Sun Y, Zboril EK, De la Chapa JJ & Singh BB (2019) Loss of Ca(2+) entry via Orai-TRPC1 induces ER stress, initiating immune activation in macrophages, Journal of cell science. 133.
75. Vaeth M, Zee I, Concepcion AR, Maus M, Shaw P, Portal-Celhay C, Zahra A, Kozhaya L, Weidinger C, Philips J, Unutmaz D & Feske S (2015) Ca2+ Signaling but Not Store-Operated Ca2+ Entry Is Required for the Function of Macrophages and Dendritic Cells, Journal of immunology. 195, 1202–17.
76. Braun A, Gessner JE, Varga-Szabo D, Syed SN, Konrad S, Stegner D, Vogtle T, Schmidt RE & Nieswandt B (2009) STIM1 is essential for Fcgamma receptor activation and autoimmune inflammation, Blood. 113, 1097–104. [PubMed: 18941110]
77. Takezawa R, Cheng H, Beck A, Ishikawa J, Launay P, Kubota H, Kinet JP, Fleig A, Yamada T & Penner R (2006) A pyrazole derivative potently inhibits lymphocyte Ca2+ influx and cytokine production by facilitating transient receptor potential melastatin 4 channel activity, Molecular pharmacology. 69, 1413–20. [PubMed: 16407466]
78. Libako P, Nowacki W, Castiglioni S, Mazur A & Maier JA (2016) Extracellular magnesium and calcium blockers modulate macrophage activity, Magnesium research. 29, 11–21. [PubMed: 27160489]
79. Martinez-Zaguilan R, Martinez GM, Lattanzio F & Gillies RJ (1991) Simultaneous measurement of intracellular pH and Ca2+ using the fluorescence of SNARF-1 and fura-2, The American journal of physiology. 260, C297–307. [PubMed: 1996613]
80. Chokshi R, Fruasaha P & Kozak JA (2012) 2-aminoethyl diphenyl borinate (2-APB) inhibits TRPM7 channels through an intracellular acidification mechanism, Channels. 6, 362–9. [PubMed: 22922232]

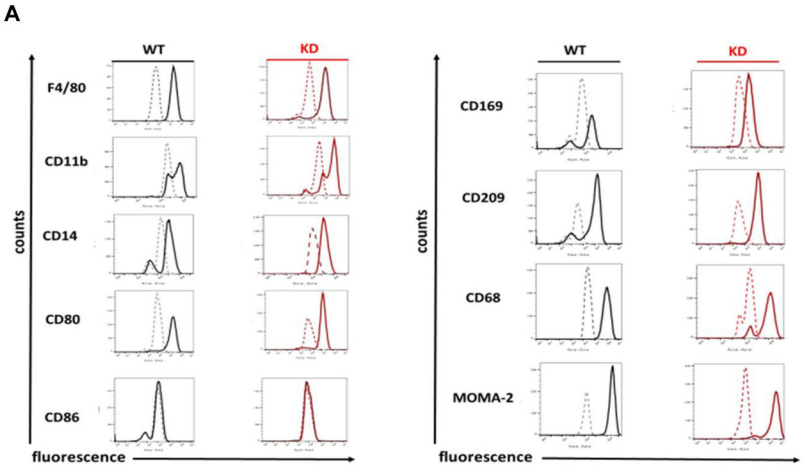

B

Marker	WT (%)	KD (%)	t-test
F4/80	97.85	88.59	**0.09**
CD11b	42.60	63.56	**0.07**
CD14	17.62	5.07	0.21
CD68	99.40	93.02	0.30
CD169	52.05	33.74	0.17
MOMA-2	99.07	99.30	0.49
CD209b	47.47	72.57	**0.06**
CD80	79.01	74.86	0.72
CD86	2.45	0.42	0.22

Fig. 1. Cell-surface and internal markers found on splenic macrophages isolated from TRPM7 KD and WT mice.

(A) FACs analysis of macrophage markers. (B) Marker expression levels expressed as a percentage. Data from (A) were collected from at least 3 WT and 3 TRPM7 KD mice. In (B) Student's t-test was performed for macrophage marker expression. The differences between macrophage marker expression levels for WT and TRPM7 KD mice were not statistically significant.

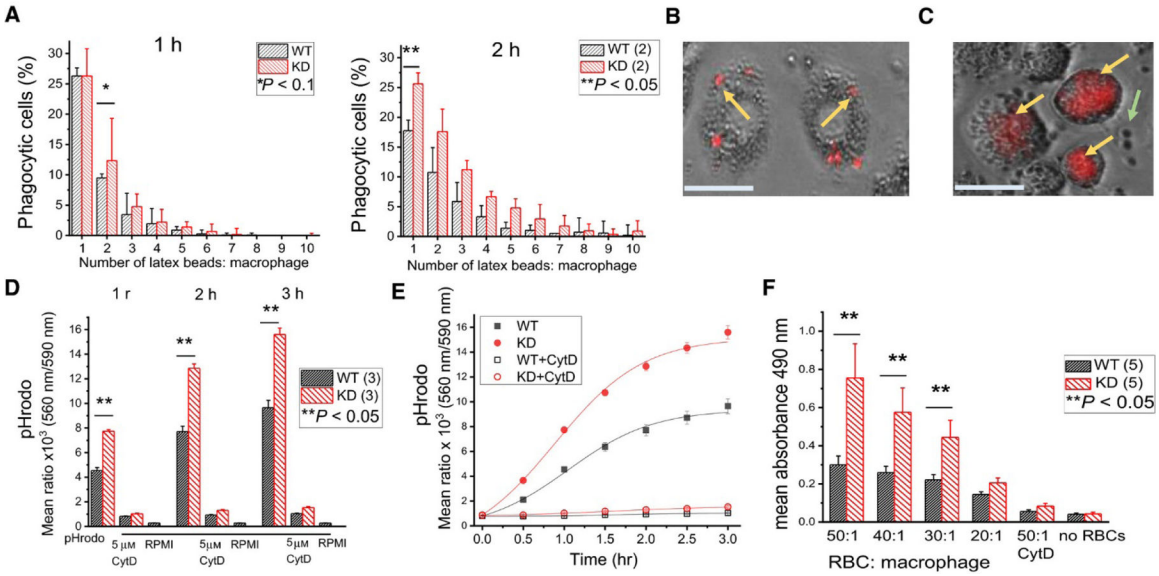

Fig. 2. TRPM7 KD murine macrophages phagocytize more efficiently than WT.

(A) Phagocytosis of latex beads after 1 and 2 h. Data collected from two WT and two KD mice. (B) Enlarged image of TRPM7 KD macrophages phagocytizing latex beads. (C) Enlarged image of TRPM7 KD macrophages phagocytizing pHrodo zymosan particles. Yellow arrows in (B) and (C) point to particles that are internalized or attached to cell surface. Green arrow in (C) shows nonphagocytized particles. Scale bars in B and C represent 25 µm. (D) Phagocytosis of pHrodo zymosan particles after 1, 2, and 3 h ± 5 µm CytD. Data collected from three WT and three KD mice. (E) Phagocytosis rate using data from (D). (F) Phagocytosis of opsonized sheep erythrocytes ± 5 µm CytD. Data collected from five WT and five KD mice. *P < 0.1, **P < 0.05, Student's t-test. Error bars represent average SEM.

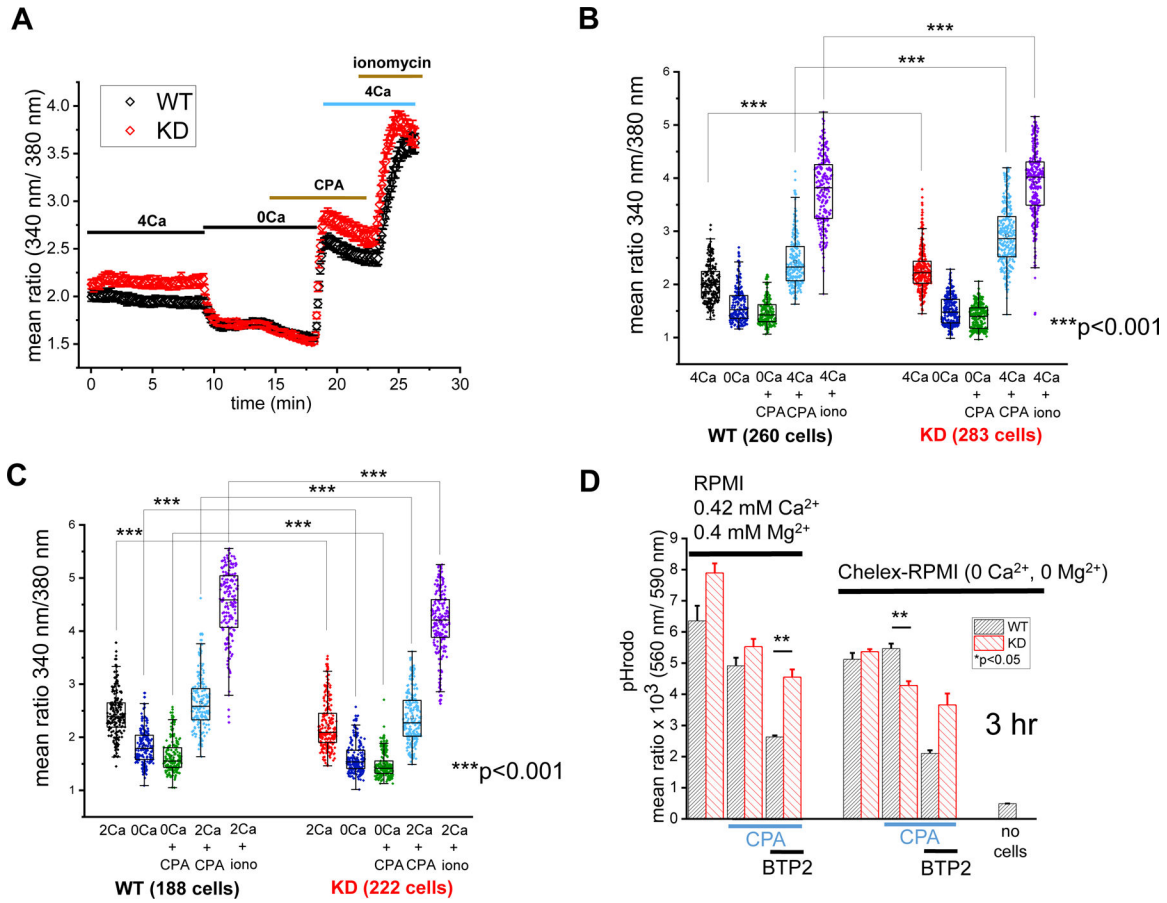

Fig. 3. Cytosolic calcium in WT and KD macrophages.

(A) The time course of intracellular Ca^{2+} levels in TRPM7 KD and WT splenic macrophages. Data in (A) are averages of cells from 4 WT and 3 KD mice. (B) Basal Ca^{2+} levels, and Ca^{2+} levels following CPA-induced store depletion and store-operated Ca^{2+} entry amplitudes in 4 mM Ca^{2+} are shown for individual cells from (A). (C) Basal Ca^{2+} levels and Ca^{2+} levels following CPA-induced store depletion and store-operated Ca^{2+} entry amplitudes in 2 mM Ca^{2+}. Data in (C) were obtained from 3 WT and 3 KD mice. **p<0.001, Student's t-test. (D) Effects of 10 μM BTP2 on phagocytosis of pHrodo zymosan particles in the presence and absence of Ca^{2+} and Mg^{2+} after 3 hours of phagocytosis. *p<0.05, Student's t test. Error bars in panels B, C, D are average S.E.M.

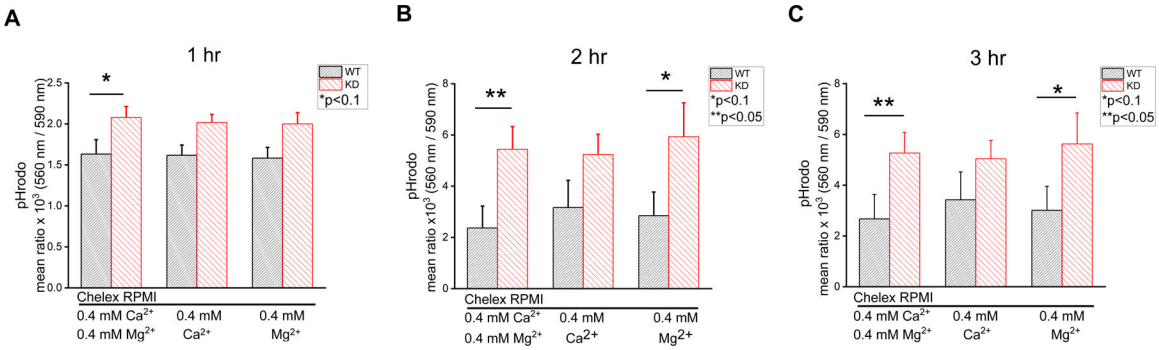

Fig. 4. Removal of Ca^{2+} and Mg^{2+} from media alters phagocytic properties of WT and TRPM7 KD macrophages.

Phagocytosis of pHrodo zymosan particles in media with and without 0.4 mM Ca^{2+} and/or Mg^{2+} after 1 hr (A), 2 hrs (B) and 3 hrs (C). Bar graphs represent mean values obtained from 4 WT and 4 KD mice. *p<0.1, **p<0.05, Student's t-test. Error bars in panels B and C are average S.E.M.

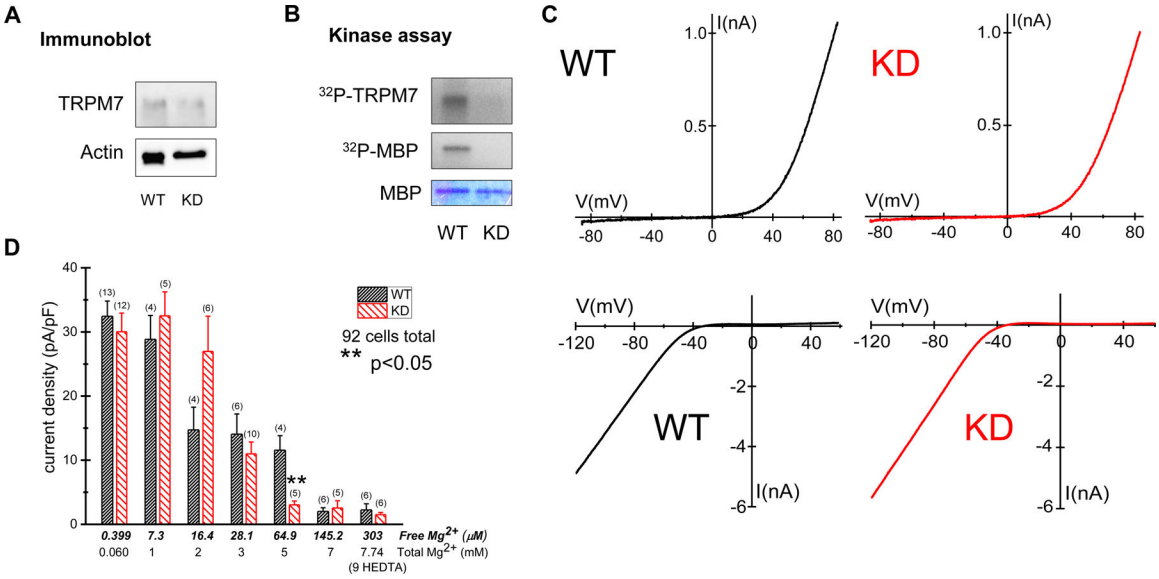

Fig. 5. Protein levels, kinase activity, current amplitudes and Mg^{2+} sensitivity of kinase-inactivated TRPM7 channels.

(A) Immunoblot analysis of immunoprecipitated TRPM7 from whole cell lysates of WT and TRPM7 KD splenic macrophages. The equal amount of protein loading was confirmed by probing for actin. (B) Incorporation of ^{32}P into MBP by TRPM7 immunoprecipitated from WT and TRPM7 KD mouse splenic macrophages. Coomassie blue staining was used to confirm equal quantities of MBP. In (A) and (B) lysates from one mouse were used for each immunoblot analysis. Similar results were obtained in three independent experiments. (C) Patch clamp electrophysiology of splenic macrophages: top panels show TRPM7 and bottom panels, inwardly rectifying K^+ channel current-voltage relations. TRPM7 current-voltage relations were obtained 5 min after recording with internal 10 mM HEDTA. (D) TRPM7 current densities at 125th ramp (~5 min) after break-in in WT and KD peritoneal macrophages. Internal solution contained 0.399 – 303 μM free Mg^{2+}, as described in Materials and Methods. Standard external solution containing 2 mM $CaCl_2$ was used. Number of cells is shown in parentheses. ** $p<0.05$: Student's t-test. Note that for 303 μM Mg^{2+} the internal solution contained 9 mM instead of 10 mM HEDTA. Error bars in D are average S.E.M.

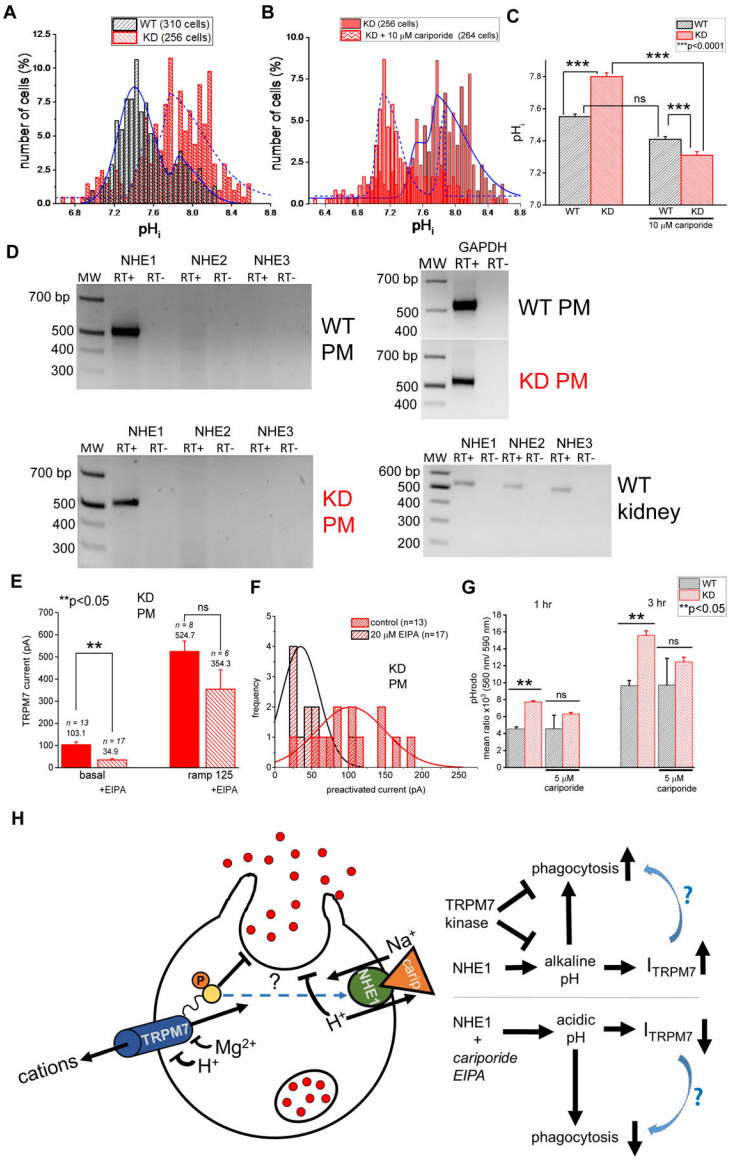

Fig. 6. Cytoplasmic pH in TRPM7 KD macrophages is alkalinized: effects of NHE1 blockade on phagocytosis and channel activity.

(A). Comparison of resting cytoplasmic pH in WT and KD splenic macrophages. (B). Effect of 10 μM cariporide on KD macrophage pHi. (C). Summary of cariporide effects on WT and KD macrophage pH_i. (D). RT-PCR of NHE1, 2, 3 in WT and KD mutant peritoneal macrophages (PM). Control: GAPDH expression in peritoneal macrophages and NHE1–3 expression in WT kidney. (E). Preactivated (basal) and maximum (ramp 125) TRPM7 current amplitudes in KD peritoneal macrophages +/− 20 μM EIPA. (F). Histograms of preactivated current amplitudes generated from the same data as in E. (G). pH rodo particle phagocytosis measured in WT and KD splenic macrophages +/− 5 μM cariporide at 1 and 3 hrs. Data are mean values from 3 WT and 3 KD mice. (H). Cartoon summary of experiments described in panels A–G and Fig. 2. TRPM7 current is shown as I_{TRPM7}. **p<0.05, ***p<0.0001, Student's t-test. Error bars in panels C, E, G are average S.E.M.